

# A Survey for Deep RGBT Tracking

Zhangyong Tang, Tianyang Xu, and Xiao-Jun Wu

**Abstract**—Visual object tracking with the visible (RGB) and thermal infrared (TIR) electromagnetic waves, shorted in RGBT tracking, recently draws increasing attention in the tracking community. Considering the rapid development of deep learning, a survey for the recent deep neural network based RGBT trackers is presented in this paper. Firstly, we give brief introduction for the RGBT trackers concluded into this category. Then, a comparison among the existing RGBT trackers on several challenging benchmarks is given statistically. Specifically, MDNet and Siamese architectures are the two mainstream frameworks in the RGBT community, especially the former. Trackers based on MDNet achieve higher performance while Siamese-based trackers satisfy the real-time requirement. In summary, since the large-scale dataset LasHeR is published, the integration of end-to-end framework, *e.g.*, Siamese and Transformer, should be further considered to fulfil the real-time as well as more robust performance. Furthermore, the mathematical meaning should be more considered during designing the network. This survey can be treated as a look-up-table for researchers who are concerned about RGBT tracking.

**Index Terms**—visual object tracking, RGBT tracking, MDNet, Siamese.

## I. INTRODUCTION

Given the first frame as the prior, visual object tracking aims at predicting a compact bounding box of the object among the whole sequence. Due to the price friendly characteristic of visible sensor, RGB tracking occupies the dominating status in the tracking community. However, current researches have noticed its shortcomings in extreme environment conditions, *e.g.*, fog and night. Basically, RGB data is imaged with the electromagnetic waves reflected by the object. Thus, it is persuasive that all the factors interfering the reflection have direct influence on the imaging procedure. On the contrary, thermal data is imaged by the emitted thermal radiations from the objects with temperature above absolute zero. Therefore, it is considered being complementary to the RGB modality. Recently, thanks to the development of RGB and TIR all-in-one equipments, the multi-modal clues can be constructed simultaneously and applied to the downstream tasks, *e.g.*, tracking [1], [2], [3], [4], image fusion [5], [6], [7], [8] and segmentation [9], [10]. In this paper, the main concentration is put on tracking with multi-modal, *i.e.*, RGBT tracking. Fig. 1 shows some pairs of RGBT data.

The rest of this paper is arranged as follows. We briefly introduce the existing deep RGBT trackers in Section II. And then their quantitative performances are compared on several benchmarks in Section III. Then the conclusion is given in the final Section V.

Z. Tang, T. Xu and X.-J. Wu are with the School of Artificial Intelligence and Computer Science, Jiangnan University, Wuxi, P.R. China. (e-mail: {zhangyong\_tang\_jnu; tianyang\_xu; xiaojun\_wu\_jnu}@163.com)



Fig. 1. An illustration of paired RGBT data. Here the sequences *i.e.*, *soccer2*, *walking40*, *womanred*, *tree5*, *balancebike*, *biketwo* are selected from RGBT210 [11]. The region in gray indicates the TIR images while the other represents images in RGB space.

## II. RGBT TRACKERS

In this section, we will introduce the mainstream frameworks employed in the RGBT tracking community.

### A. MDNet-based RGBT Trackers

MDNet [12], which is the champion of VOT-2015 challenge [13], treats each sequence as a single domain and uses the online updating technique to acquire the object-specific clues, obtaining robust tracking performance. Thus, lots of RGBT trackers based on MDNet, which are presented in TABLE I, is proposed. And Fig 2 shows the basic extension of MDNet in RGBT tracking. Generally, the feature extractor and fusion module are trained offline while the last fully-connected layer is trained online. For example, at the beginning of the tracking procedure of 'Sequence 1', the first frame is utilized to train the parameters of the last fully-connected layer, giving more object-specific consideration.

Since the tracking process is generally similar, the main discrepancy of different algorithms lies in the feature extractor and fusion module, especially the latter. Thus, we mainly

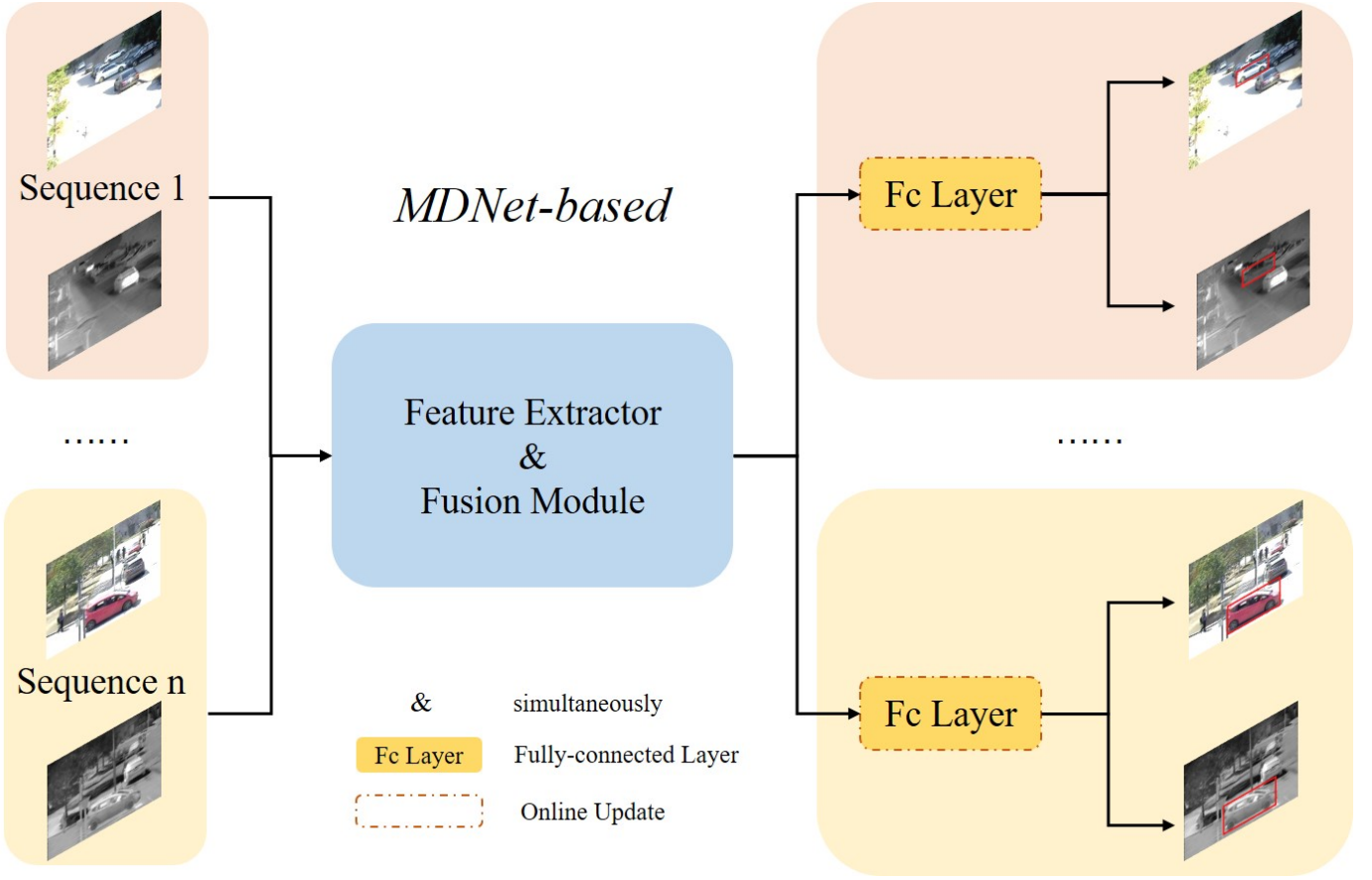


Fig. 2. Pipeline of MDNet-based RGBT trackers. The processes of feature extraction and multi-modal fusion are completed in the first blue block. And the block rendered in yellow is the last fully-connected (Fc) layer, which is online initialized before the tracking procedure.

focus on the fusion modules of the methods described below. In FANet [14], the feature channels from both RGB and TIR modalities are firstly concatenated for inter-modality interactions and then separated for fusion weights calculating, which is normalized by a Softmax operator applied in a cross-modal way. DAPNet [15] achieves the fusion task by recurrently using a sub-network, which consists of a convolutional layer, a Rectified Linear Unit (ReLU) activation [16] and a normalization layer, at different feature levels. Compared with the coarse fusion sub-network used in DAPNet, DAFNet [17] further designs an adaptive fusion module which is similar to that in FANet. Carefully programmed, MANet [18] expects to extract the modality-specific, modality-shared and object-specific clues through modality, generator and instance adapters respectively. [19] investigates the potential of attention mechanism in RGBT tracking, *i.e.*, local attention for offline training and global attention for online testing. Similarly, CMPP [20] employs the attention mechanism to finish the inter-modality correlation which is further extended to the temporal dimensional due to the significance of temporal information in video analysis. A duality-gated mutual conditional module aims to achieve the multi-modal fusion task in a mutual-guided way in DMCNet [21]. Based on MANet, the features formerly enhanced within each modality before the fusion stage in MANet++ [22]. A quality-aware fusion block

is constructed to evaluate the modality significance in CBPNet [23]. Aiming at strengthen the stronger modality and suppress the weaker modality, a lightweight attention-based fusion module is applied in M<sup>5</sup>L [24]. All the above trackers mentioned in this sub-section maintain a fused feature representation after the cross-modal interactions. However, to keep the modality-specific characteristics being discriminative, the features from RGB and TIR modalities are also retained in some methods. Specifically, MacNet [25] learns the fusion weights through the independent modal-aware attention network and competitive learning [26], for which the features of RGB and TIR modalities are reserved, leverages the capacity of results from single modality and the modality-fused branch. TFNet [27] deploys a trident branch architecture and each branch is specific for the RGB, TIR and fused features. Different from the most existing RGBT trackers, CAT [28], ADRNet [29] and APFNet [30] make their network construction more concrete for both modality-specific (*e.g.*, illumination variation in RGB and thermal crossover in TIR) and modality-shared (*e.g.*, scale variation) challenges. In CAT [28], all the challenge-specific features are adaptively aggregated and then complemented to the basic learning procedure of both modalities. ADRNet [29] designs an attribute-driven residual block to measure the appearance model under different circumstance and then all the information is ensembled before the residual connection to the

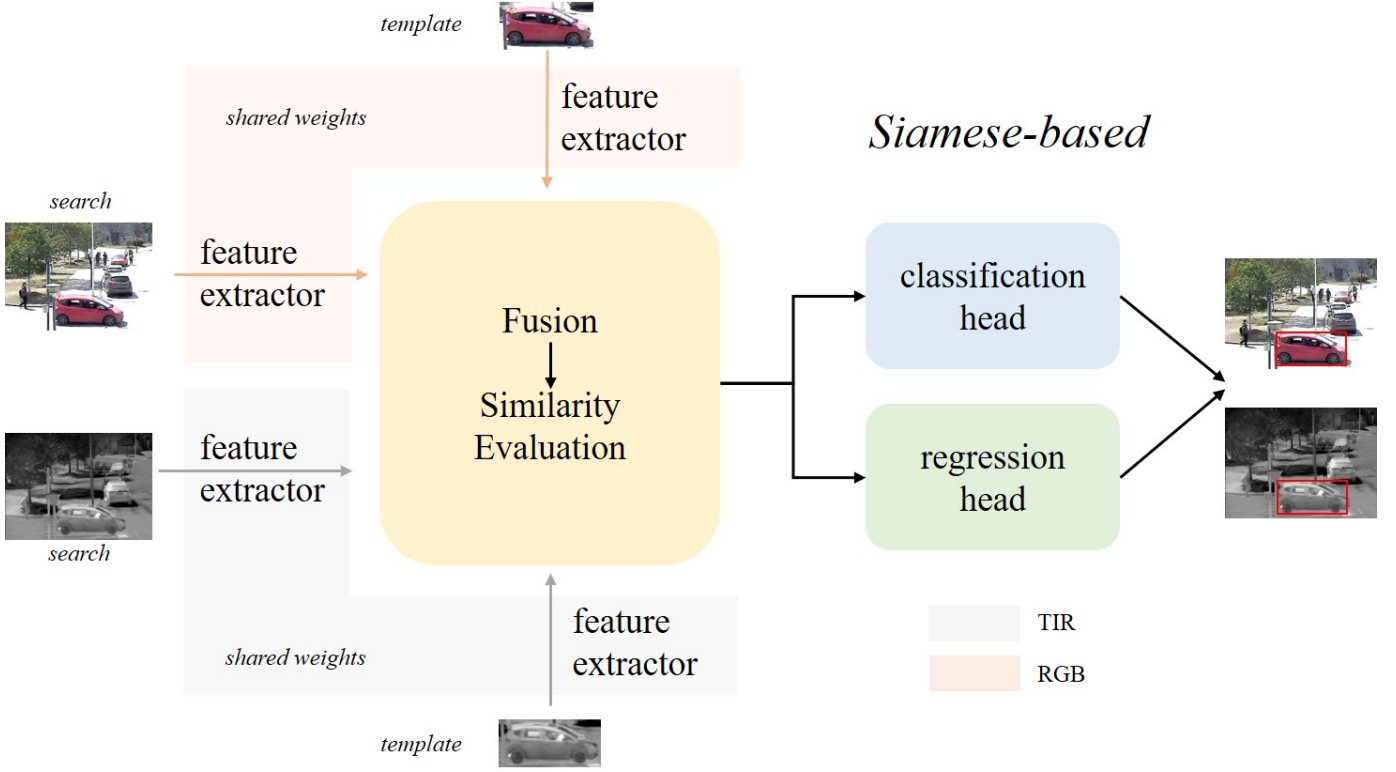


Fig. 3. Pipeline of the published Siamese-based RGBT trackers. For fusion at feature level, the multi-modal fusion locates between the feature extraction and similarity evaluation. For pixel-level and decision-level fusion, the network architecture always degrades to a single-modality configuration and, therefore, it is not included in this figure.

basic learned feature representation. Similarly, in APFNet [30], the aggregated multi-challenge features are combined with the features solely learned from RGB or TIR modality through transformer encoder and decoder blocks.

### B. Siamese-based RGBT Trackers

In visual object tracking, Siamese network is carried forward by the pioneering work SiamFC [31] due to its efficiency brought by the end-to-end training scheme. Totally, it aims to learn a general similarity evaluation metric and its pipeline is shown in Fig 3. As the figure shows, the existing Siamese-based trackers employ unequal feature extractors for RGB and TIR modalities. Then, in the published Siamese-based RGBT trackers, the multi-modal fusion module is followed to achieve the feature aggregation. After that, the same strategy for similarity evaluation is applied for both classification and regression before their corresponding heads.

Since the core of multi-modal task lies in the combination of multi-modal clues, the fusion mechanism is mainly described for the following methods. At the beginning, the thermal data is employed by replacing one of the channels of RGB data in [32]. Treating the SiamFC [31] as the baseline, SiamFT [33] uses simple concatenation for the features of template inputs while these of search inputs are fused by the learned modality reliabilities. Based on SiamFT, the dynamic online-learned transformation strategy as well as the multi-level semantic features are further employed in DSiamMFT [34]. Similarly to [32], fusion at the input stage, DuSiamRT [35]

utilizes modality-wise channel attention mechanism to fuse the features of template inputs while keeps unchanged for the features of search inputs. SiamCDA [36], whose baseline tracker is an advanced anchor-based tracker, *i.e.*, SiamRPN++ [37], introduces the information from one modality to the other modality through the generated weights. Furthermore, to cope with the situation at that time that there exists insufficient annotated RGBT data for large-scale network training, the LSS Dataset<sup>1</sup> is synthesized in a statistical way which contributes to its superior performance.

### C. Other Deep RGBT Trackers

Except the MDNet-based and Siamese-based framework mentioned before, some RGBT trackers are built based on other frameworks. In [38], the multi-modal information is straightforwardly combined by addition. mFDiMP [39] is the tracker based on DiMP [40] which is a superior RGB tracker that many researchers follow. Specifically, DiMP is extended to the TIR modality and a TIR dataset is generated from GOT10k [41] and employed for the learning of neural network. JMMAC [42], who is the champion of the published datasets of the VOT-RGBT2019 [43] and VOT-RGBT2020 [44], learns the fusion weights through two sub-networks for local and global attention respectively.

<sup>1</sup><https://github.com/RaymondCover/LSS-Dataset>

TABLE I  
A COLLECTION OF THE EXISTING DEEP RGBT TRACKERS.

Trackers	Baseline	Year	Published	Reference
-	Others	2018	NeuroComputing	[38]
mfDiMP	Others	2019	ICCVW	[39]
MANet	MDNet-based	2019	ICCVW	[18]
DAPNet	MDNet-based	2019	ACM MM	[15]
DAFNet	MDNet-based	2019	ICCVW	[17]
-	MDNet-based	2019	ICIP	[19]
-	Siamese-based	2019	FUSION	[32]
SiamFT	Siamese-based	2019	IEEE Access	[33]
MaCNet	MDNet-based	2020	Sensors	[25]
DMCNet	MDNet-based	2020	arXiv	[21]
CMPP	MDNet-based	2020	CVPR	[20]
CAT	MDNet-based	2020	ECCV	[28]
DSiamMFT	Siamese-based	2020	Signal Processing: Image Communication	[34]
JMMAC	Others	2021	IEEE TIP	[42]
MANet++	MDNet-based	2021	IEEE TIP	[22]
CBPNet	MDNet-based	2021	IEEE TMM	[23]
TFNet	MDNet-based	2021	IEEE TCSVT	[27]
FANet	MDNet-based	2021(2018)	IEEE TIV(arXiv)	[14]
ADNet	MDNet-based	2021	IJCV	[29]
M <sup>5</sup> L	MDNet-based	2021	IEEE TIP	[24]
SiamCDA	Siamese-based	2021	IEEE TCSVT	[36]
DuSiamRT	Siamese-based	2021	The Visual Computer	[35]
APFNet	MDNet-based	2022	AAAI	[30]

### III. DATASETS AND RESULTS

In this section, we will firstly give a introduction to the existing RGBT dataset, *i.e.*, GTOT [45], RGBT210 [11], RGBT234 [46], VOT-RGBT2019 [43], VOT-RGBT2020 [44] and LasHeR [47]. After that, a comparison of the existing deep RGBT trackers on multi-benchmarks will be listed and analysed.

#### A. Datasets and Evaluation Metrics

TABLE II shows the detail information about these six benchmarks. Here 'Num of Sequences' represents the number of paired RGBT videos. 'Aligned' means whether the RGB and TIR images are aligned or not. Specifically, if there exists one groundtruth file ('Y'), the RGB and TIR modalities are thought aligned. It should be noticed that the VOT-RGBT2019 dataset is a sub-set of RGBT234 and the difference between VOT-RGBT2019 and VOT-RGBT2020 benchmarks locate in the testing protocol. Therefore, they are the same in statistic analysis [44].

The same evaluation metrics are employed in GTOT [45], RGBT210 [11], RGBT234 [46] and LasHeR [47] datasets, *i.e.*, Precision and Success. Precision rate measures the distance between the groundtruth bounding box and the predicted one. Success rate represents the ratio of tracking failures whose Intersection over Union (IoU) between its corresponding label below a given threshold.

Accuracy, Robustness and (Excepted Average Overlap) EAO are the measurements utilized in VOT-RGBT2019 [43] and VOT-RGBT2020 [44]. The overlap between the prediction

and the groundtruth is represented by accuracy. Robustness is designed to measure the ratio of tracking failures over the total numbers of image frames. EAO is considered the most important and comprehensively indicates the superiority of the tracker.

#### B. Results

TABLE III shows the results on GTOT [45], RGBT210 [11], RGBT234 [46] and LasHeR [47] while the results on the VOT benchmarks are exhibited in TABLE IV. On GTOT, the highest Success rate is obtained by ADNet [29] and APFNet [30] (0.739) while the best Precision rate reaches 0.926 by CMPP [20]. On RGBT210, DMCNet [21] achieves the best Precision (0.797) and Success (0.555) rates at the same time. Consistently, DMCNet also ranks the first on Precision (0.839) and Success (0.593) rates on RGBT234 dataset. APFNet [30] gets the best Precision and Success scores on LasHeR dataset. For the VOT benchmarks, as mentioned before, JMMAC [42] ranks the first on the public dataset twice. However, the VOT community provides one public dataset combined with a sequestered one, and the real champion is decided on the private dataset. The champion of VOT-RGBT2019 [43] is mfDiMP [39] and DFAT wins the VOT-RGBT2020 challenge [44].

### IV. DISCUSSION

From the above investigations, we have several discussions as follows: (1) Following the whole computer vision field, the potential of Transformer model [48] is not explored yet.



TABLE II  
ILLUSTRATION FOR RGBT DATASETS (ONLY FOR TESTING).

Benchmark	Year	Num of Sequences	Aligned	Category	Num of attributes	Reference
GTOT	2016	50	N	9	7	[45]
RGBT210	2017	210	Y	22	12	[11]
RGBT234	2019	234	N	22	12	[46]
VOT-RGBT2019	2019	60	-	13	12	[43]
VOT-RGBT2020	2019	60	-	13	12	[44]
LasHeR	2021	245	Y	32	19	[47]

TABLE III  
QUANTITATIVE RESULTS OF THE EXISTING DEEP RGBT TRACKERS ON GTOT, RGBT210, RGBT234 AND LASHER DATASETS.

Trackers	GTOT [45]		RGBT210 [11]		RGBT234 [46]		LasHeR [47]	
	Precision(↑)	Success(↑)	Precision(↑)	Success(↑)	Precision(↑)	Success(↑)	Precision(↑)	Success(↑)
[38]	0.852	0.626	-	-	-	-	-	-
mfDiMP [39]	-	-	0.786	0.555	0.785	0.559	0.447	0.344
MANet [18]	0.894	0.724	-	-	0.777	0.539	0.457	0.33
DAPNet [15]	0.882	0.707	-	-	0.766	0.537	0.431	0.314
DAFNet [17]	0.891	0.712	-	-	0.796	0.544	0.449	0.311
[19]	0.843	0.677	-	-	0.787	0.545	-	-
[32]	-	-	-	-	0.610	0.428	-	-
SiamFT [33]	0.826	0.700	-	-	0.688	0.486	-	-
MaCNet [25]	0.880	0.714	-	-	0.790	0.554	0.483	0.352
DMCNet [21]	0.909	0.733	0.797	0.555	0.839	0.593	0.491	0.357
CMPP [20]	0.926	0.738	-	-	0.823	0.575	-	-
CAT [28]	0.889	0.717	0.792	0.533	0.804	0.561	0.451	0.317
DSiamMFT [34]	-	-	0.642	0.432	-	-	-	-
JMMAC [42]	0.902	0.732	-	-	0.790	0.573	-	-
MANet++ [22]	0.901	0.723	-	-	0.800	0.554	0.467	0.317
CBPNet [23]	0.885	0.716	-	-	0.794	0.541	-	-
TFNet [27]	0.886	0.729	0.777	0.529	0.806	0.560	-	-
FANet [14]	0.891	0.728	-	-	0.787	0.553	0.442	0.309
ADRNet [29]	0.904	0.739	-	-	0.809	0.571	-	-
M <sup>5</sup> L [24]	0.896	0.710	-	-	0.795	0.542	-	-
SiamCDA [36]	0.877	0.732	-	-	0.760	0.569	-	-
DuSiamRT [35]	0.766	0.628	-	-	0.567	0.384	-	-
APFNet [30]	0.905	0.739	-	-	0.827	0.579	0.500	0.362

(2) Different the image-based tasks [49], [50], [51], [5], [52], [53], [54], [55], [56], tempoal information , which has not been widely studied in RGBT tracking yet, is of great inportance in video-based tasks, *e.g.*, visual object tracking.  
(3) During the investigation, we find that less mathematical theories considered during the network construction process.  
(4) Behind the fusion step, what is actually going on has not been discussed yet. In the future, we will mainly focus on more concrete RGBT tracking based on our discussions.

## V. CONCLUSION

In this paper, a statistic analysis of the existing deep RGBT trackers. Specifically, all the trackers are divided into three categories, *i.e.*, MDNet-based, Siamese-based and Others. Furthermore, their quantitative results on GTOT, RGBT210, RGBT234, LasHeR, VOT-RGBT2019 and VOT-RGBT2020

benchmarks are compared intuitively by gathering them together. Therefore, this work can act like a reference for researchers who are interested in RGBT tracking.

## REFERENCES

- [1] X.-F. Zhu, X.-J. Wu, T. Xu, Z.-H. Feng, and J. Kittler, "Complementary discriminative correlation filters based on collaborative representation for visual object tracking," *IEEE Transactions on Circuits and Systems for Video Technology*, vol. 31, no. 2, pp. 557–568, 2020.
- [2] X. Zhu, X.-J. Wu, T. Xu, Z.-H. Feng, and J. Kittler, "Complementary discriminative correlation filters based on collaborative representation for visual object tracking," *IEEE Transactions on Circuits and Systems for Video Technology*, vol. 31, no. 2, pp. 557–568, 2021.
- [3] T. Xu, Z. Feng, X. Wu, and J. Kittler, "Learning adaptive discriminative correlation filters via temporal consistency preserving spatial feature selection for robust visual object tracking," *IEEE Transactions on Image Processing*, vol. 28, no. 11, pp. 5596–5609, 2019.
- [4] T. Xu, Z. Feng, X. Wu, and J. Kittler, "Joint group feature selection and discriminative filter learning for robust visual object tracking," in *2019 IEEE/CVF International Conference on Computer Vision (ICCV)*, 2019, pp. 7949–7959.

TABLE IV  
QUANTITATIVE RESULTS ON VOT-RGBT2019 AND VOT-RGBT2020 DATASETS.

Trackers	VOT-RGBT2019 [43]			VOT-RGBT2020 [44]		
	Accuracy( $\uparrow$ )	Robustness( $\uparrow$ )	EAO( $\uparrow$ )	Accuracy( $\uparrow$ )	Robustness( $\uparrow$ )	EAO( $\uparrow$ )
mfDiMP [39]	0.6019	0.8036	0.3879	0.6380	0.7930	0.3800
MANet [18]	0.5823	0.7010	0.3463	-	-	-
SiamFT [33]	0.6300	0.6390	0.3100	-	-	-
MaCNet [25]	0.5451	0.5914	0.3052	-	-	-
JMMAC [42]	0.6649	0.8211	0.4826	0.6620	0.8180	0.4200
MANet++ [22]	0.5092	0.5379	0.2716	-	-	-
TFNet [27]	0.4617	0.5936	0.2878	-	-	-
FANet [14]	0.4724	0.5078	0.2465	-	-	-
ADRNet [29]	0.6218	0.7657	0.3959	-	-	-
SiamCDA [36]	0.6820	0.7570	0.4240	-	-	-

- [5] H. Li, X.-J. Wu, and T. Durrani, "Nestfuse: An infrared and visible image fusion architecture based on nest connection and spatial/channel attention models," *IEEE Transactions on Instrumentation and Measurement*, vol. 69, no. 12, pp. 9645–9656, 2020.
- [6] X. Luo, Z. Zhang, B. Zhang, and X.-J. Wu, "Image fusion with contextual statistical similarity and nonsubsampling shearlet transform," *IEEE Sensors Journal*, vol. 17, no. 6, pp. 1760–1771, 2017.
- [7] H. Li and X.-J. Wu, "Multi-focus image fusion using dictionary learning and low-rank representation," in *International Conference on Image and Graphics*. Springer, Cham, 2017, pp. 675–686.
- [8] X. Luo, Z. Zhang, and X. Wu, "A novel algorithm of remote sensing image fusion based on shift-invariant shearlet transform and regional selection," *AEU-International Journal of Electronics and Communications*, vol. 70, no. 2, pp. 186–197, 2016.
- [9] C. Li, L. Lin, W. Zuo, S. Yan, and J. Tang, "Sold: Sub-optimal low-rank decomposition for efficient video segmentation," in *2015 IEEE Conference on Computer Vision and Pattern Recognition (CVPR)*, 2015, pp. 5519–5527.
- [10] C. Li, L. Lin, W. Zuo, W. Wang, and J. Tang, "An approach to streaming video segmentation with sub-optimal low-rank decomposition," *IEEE Transactions on Image Processing*, vol. 25, no. 5, pp. 1947–1960, 2016.
- [11] C. Li, N. Zhao, Y. Lu, C. Zhu, and J. Tang, "Weighted sparse representation regularized graph learning for rgb-t object tracking," in *Proceedings of the 25th ACM International Conference on Multimedia*, 2017, p. 1856–1864.
- [12] H. Nam and B. Han, "Learning multi-domain convolutional neural networks for visual tracking," in *2016 IEEE/CVF Conference on Computer Vision and Pattern Recognition (CVPR)*, 2016, pp. 4293–4302.
- [13] M. Kristan, J. Matas, and A. et.al, "The visual object tracking vot2015 challenge results," in *Visual Object Tracking Workshop 2015 at ICCV2015*, Dec 2015.
- [14] Y. Zhu, C. Li, J. Tang, and B. Luo, "Quality-aware feature aggregation network for robust rgbt tracking," *IEEE Transactions on Intelligent Vehicles*, vol. 6, no. 1, pp. 121–130, 2021.
- [15] Y. Zhu, C. Li, B. Luo, J. Tang, and X. Wang, "Dense feature aggregation and pruning for rgbt tracking," in *Proceedings of the 27th ACM International Conference on Multimedia*, 2019, pp. 465–472.
- [16] X. Glorot, A. Bordes, and Y. Bengio, "Deep sparse rectifier neural networks," in *Proceedings of the Fourteenth International Conference on Artificial Intelligence and Statistics, AISTATS 2011*, 2011, pp. 315–323.
- [17] Y. Gao, C. Li, Y. Zhu, J. Tang, T. He, and F. Wang, "Deep adaptive fusion network for high performance rgbt tracking," in *2019 IEEE/CVF International Conference on Computer Vision Workshop (ICCVW)*, 2019, pp. 91–99.
- [18] C. L. Li, A. Lu, A. H. Zheng, Z. Tu, and J. Tang, "Multi-adapter rgbt tracking," in *2019 IEEE/CVF International Conference on Computer Vision Workshop (ICCVW)*, 2019, pp. 2262–2270.
- [19] R. Yang, Y. Zhu, X. Wang, C. Li, and J. Tang, "Learning target-oriented dual attention for robust rgb-t tracking," in *2019 IEEE International Conference on Image Processing (ICIP)*, 2019, pp. 3975–3979.
- [20] C. Wang, C. Xu, Z. Cui, L. Zhou, and J. Yang, "Cross-modal pattern-propagation for rgb-t tracking," in *2020 IEEE/CVF Conference on Computer Vision and Pattern Recognition (CVPR)*, 2020.
- [21] A. Lu, C. Qian, C. Li, J. Tang, and L. Wang, "Duality-gated mutual condition network for RGBT tracking," *CoRR*, vol. abs/2011.07188, 2020.
- [22] A. Lu, C. Li, Y. Yan, J. Tang, and B. Luo, "Rgbt tracking via multi-adapter network with hierarchical divergence loss," *IEEE Transactions on Image Processing*, vol. 30, pp. 5613–5625, 2021.
- [23] Q. Xu, Y. Mei, J. Liu, and C. Li, "Multimodal cross-layer bilinear pooling for rgbt tracking," *IEEE Transactions on Multimedia*, pp. 1–1, 2021.
- [24] Z. Tu, C. Lin, W. Zhao, C. Li, and J. Tang, "M<sub>sup</sub>/S<sub>sup</sub>: Multi-modal multi-margin metric learning for rgbt tracking," *IEEE Transactions on Image Processing*, vol. 31, pp. 85–98, 2022.
- [25] H. Zhang, L. Zhang, L. Zhuo, and J. Zhang, "Object tracking in rgb-t videos using modal-aware attention network and competitive learning," *Sensors*, vol. 20, no. 2, p. 393, 2020.
- [26] D. E. Rumelhart and J. L. McClelland, in *MIT Press*, 1987.
- [27] Y. Zhu, C. Li, J. Tang, B. Luo, and L. Wang, "Rgbt tracking by trident fusion network," *IEEE Transactions on Circuits and Systems for Video Technology*, pp. 1–1, 2021.
- [28] C. Li, L. Liu, A. Lu, Q. Ji, and J. Tang, "Challenge-aware rgbt tracking," in *European Conference on Computer Vision (ECCV)*. Springer International Publishing, 2020, pp. 222–237.
- [29] H. L. Pengyu Zhang, Dong Wang and X. Yang, "Learning Adaptive Attribute-Driven Representation for Real-Time RGB-T Tracking," *International Journal of Computer Vision*, vol. 129, pp. 2714–2729, 2021.
- [30] X. Yun, Y. Mengmeng, L. Chenglong, L. Lei, and T. Jin, "Attribute-based progressive fusion network for rgbt tracking," in *AAAI*, 2022.
- [31] L. Bertinetto, J. Valmadre, J. F. Henriques, A. Vedaldi, and P. H. S. Torr, "Fully-convolutional siamese networks for object tracking," in *European Conference on Computer Vision workshops*, 2016, pp. 850–865.
- [32] X. Zhang, P. Ye, D. Qiao, J. Zhao, S. Peng, and G. Xiao, "Object fusion tracking based on visible and infrared images using fully convolutional siamese networks," in *2019 22th International Conference on Information Fusion (FUSION)*, 2019, pp. 1–8.
- [33] X. Zhang, P. Ye, S. Peng, J. Liu, K. Gong, and G. Xiao, "Siamft: An rgb-infrared fusion tracking method via fully convolutional siamese networks," *IEEE Access*, vol. 7, pp. 122 122–122 133, 2019.
- [34] X. Zhang, P. Ye, S. Peng, J. Liu, and G. Xiao, "Dsiamft: An rgb-t fusion tracking method via dynamic siamese networks using multi-layer feature fusion," *Signal Processing: Image Communication*, vol. 84, p. 115756, 2020.
- [35] C. Guo, D. Yang, C. Li, and P. Song, "Dual siamese network for rgbt tracking via fusing predicted position maps," *The Visual Computer*, pp. 1–13, 2021.
- [36] T. Zhang, X. Liu, Q. Zhang, and J. Han, "Siamcda: Complementarity-and distractor-aware rgb-t tracking based on siamese network," *IEEE Transactions on Circuits and Systems for Video Technology*, pp. 1–1, 2021.
- [37] B. Li, W. Wu, Q. Wang, F. Zhang, J. Xing, and J. Yan, "Siamrpn++: Evolution of siamese visual tracking with very deep networks," in *2019 IEEE/CVF Conference on Computer Vision and Pattern Recognition (CVPR)*, 2019, pp. 4277–4286.

- [38] Chenglong, Xiaohao, Zhao, Nan, Cao, Xiaochun, Tang, and Jin, "Fusing two-stream convolutional neural networks for rgb-t object tracking," *Neurocomputing*, 2018.
- [39] L. Zhang, M. Danelljan, A. Gonzalez-Garcia, J. van de Weijer, and F. Shahbaz Khan, "Multi-modal fusion for end-to-end rgb-t tracking," in *2019 IEEE/CVF International Conference on Computer Vision Workshop (ICCVW)*, 2019, pp. 2252–2261.
- [40] G. Bhat, M. Danelljan, L. V. Gool, and R. Timofte, "Learning discriminative model prediction for tracking," in *2019 IEEE/CVF International Conference on Computer Vision, ICCV*. IEEE, 2019, pp. 6181–6190.
- [41] L. Huang, X. Zhao, and K. Huang, "Got-10k: A large high-diversity benchmark for generic object tracking in the wild," *IEEE Transactions on Pattern Analysis and Machine Intelligence*, vol. 43, no. 5, pp. 1562–1577, 2021.
- [42] P. Zhang, J. Zhao, C. Bo, D. Wang, H. Lu, and X. Yang, "Jointly modeling motion and appearance cues for robust rgb-t tracking," *IEEE Transactions on Image Processing*, vol. 30, pp. 3335–3347, 2021.
- [43] M. Kristan, J. Matas, A. Leonardis *et al.*, "The seventh visual object tracking vot2019 challenge results," in *2019 IEEE/CVF International Conference on Computer Vision Workshop (ICCVW)*, 2019, pp. 2206–2241.
- [44] M. Kristan, A. Leonardis, J. Matas, M. Felsberg, R. P. Pflugfelder, J. Kämäräinen, and M. Danelljan, "The eighth visual object tracking VOT2020 challenge results," in *European Conference on Computer Vision Workshops (ECCVW)*, vol. 12539, 2020, pp. 547–601.
- [45] C. Li, H. Cheng, S. Hu, X. Liu, J. Tang, and L. Lin, "Learning collaborative sparse representation for grayscale-thermal tracking," *IEEE Transactions on Image Processing*, vol. 25, no. 12, pp. 5743–5756, 2016.
- [46] C. Li, X. Liang, Y. Lu, N. Zhao, and J. Tang, "Rgb-t object tracking: Benchmark and baseline," *Pattern Recognition*, vol. 96, p. 106977, 2019.
- [47] C. Li, W. Xue, Y. Jia, Z. Qu, B. Luo, J. Tang, and D. Sun, "Lasher: A large-scale high-diversity benchmark for rgbt tracking," *IEEE Transactions on Image Processing*, vol. 31, pp. 392–404, 2022.
- [48] A. Vaswani, N. Shazeer, N. Parmar, J. Uszkoreit, L. Jones, A. N. Gomez, L. Kaiser, and I. Polosukhin, "Attention is all you need," *arXiv*, 2017.
- [49] C. Li, W. Yuan, A. Bovik, and X. Wu, "No-reference blur index using blur comparisons," *Electronics letters*, vol. 47, no. 17, pp. 962–963, 2011.
- [50] S.-G. Chen and X.-J. Wu, "A new fuzzy twin support vector machine for pattern classification," *International Journal of Machine Learning and Cybernetics*, vol. 9, no. 9, pp. 1553–1564, 2018.
- [51] Y.-J. Zheng, J.-Y. Yang, J. Yang, X.-J. Wu, and Z. Jin, "Nearest neighbour line nonparametric discriminant analysis for feature extraction," *Electronics Letters*, vol. 42, no. 12, pp. 679–680, 2006.
- [52] Z.-H. Feng, J. Kittler, M. Awais, P. Huber, and X.-J. Wu, "Face detection, bounding box aggregation and pose estimation for robust facial landmark localisation in the wild," in *Proceedings of the IEEE conference on computer vision and pattern recognition workshops*, 2017, pp. 160–169.
- [53] X.-J. Wu, J. Kittler, J.-Y. Yang, M. Kieron, and S. Wang, "A new direct lda (d-lda) algorithm for feature extraction in face recognition," in *Proceedings of the 17th International Conference on Pattern Recognition, 2004. ICPR 2004.*, vol. 4. IEEE, 2004, pp. 545–548.
- [54] J. Sun, C. Li, X.-J. Wu, V. Palade, and W. Fang, "An effective method of weld defect detection and classification based on machine vision," *IEEE Transactions on Industrial Informatics*, vol. 15, no. 12, pp. 6322–6333, 2019.
- [55] M. Wang, S. Wang, and X.-J. Wu, "Initial results on fuzzy morphological associative memories," *Journal of Electronics*, vol. 31, no. 005, pp. 690–693, 2003.
- [56] J. Sun, W. Fang, and X.-J. Wu, "Quantum-behaved particle swarm optimization: principle and applications," 2011.